Journal of Power Sources 185 (2008) 1478–1483

Contents lists available at ScienceDirect

Journal of Power Sources

journal homepage: www.elsevier.com/locate/jpowsour

The intelligent automotive battery, "CYBOX®"

Keizo Yamada[a,*], Yoshifumi Yamada[a], Koji Otsu[a], Yoshiaki Machiyama[a], Akihiko Emori[b], Teturo Okoshi[a]

[a] Shin-Kobe Electric Machinery Co., Ltd., 2200 Oka, Fukaya, Saitama 369-0297, Japan
[b] Hitachi Research Laboratory, Hitachi Ltd., 7-1-1 Omika, Hitachi, Ibaraki 319-1292, Japan

ARTICLE INFO

Article history:
Received 27 March 2008
Received in revised form 29 May 2008
Accepted 4 June 2008
Available online 16 July 2008

Keywords:
Intelligent battery
State of charge
State of health
Lead-acid battery
Monitoring

ABSTRACT

An intelligent battery to monitor battery states for an automotive use was newly developed. A main parameter to monitor battery states are based on the measurement of voltage variations that are to fluctuate immediately after an engine ignition. The developed monitoring unit is embedded into the lead-acid battery "CYBOX®" which does not have a current monitoring unit. The monitoring unit that has an alarm system which is compact and highly reliable essentially diagnoses the state of charge and the state of health of battery states in order to inform automotive user of the adequate timing of replace, recharge, and the hazardous state of overcharge of batteries. The battery-monitoring unit has an optical data transfer system to extract internal data from external device. The battery-monitoring unit also has a data acquisition instrument which receives more detailed monitored historical data from the optical data transfer system of the monitoring unit.

1. Introduction

Various automotive systems have been developed to improve security and driving comfort ability and achieve environmental benefit of reducing greenhouse gas emissions and fossil fuel consumption. Prominent examples of the systems using lead-acid batteries are the idling stop, the mild hybrids, and the so-called x-by-wire systems. To operate these system properly, battery characteristics also have been expected to be improved extensively. These improved batteries rely on technologies [1–5] for the highly precise detection of the state of charge and state of health to conserve the engine-start capability in idling stop, the energy regeneration during braking, and other functions of new vehicle systems [6]. In vehicles with conventional automotive systems, meanwhile, car manufacturers are introducing more electronic auto parts to increase comfort for drivers. As more of these parts are added, the battery bears increasing loads and becomes all the more indispensable for the vehicle overall [7]. Given that one-quarter of all car troubles are caused by batteries, the industry has much to gain from the prompt introduction of systems to monitor battery conditions (battery-monitoring systems) and the dissemination of those systems in the battery market. Shin-Kobe has studied a battery-monitoring technology with the plan of promptly developing a battery-monitoring system.

The important parameters for the assessment of battery conditions are the state of charge (SOC) and state of health (SOH). SOC and SOH are defined as follows:

$$\mathrm{SOC} = 100 \times \frac{\text{residual capacity}}{\text{full capacity}} \quad (1)$$

$$\mathrm{SOH} = 100 \times \frac{\text{full capacity}}{\text{initial full capacity}} \quad (2)$$

SOC can be determined in terms of a fully stabilized open-circuit voltage (OCV), and the most precise method for determining SOH is to measure a direct-current internal resistance of the battery at engine start-up [6]. The direct-current internal resistance can be measured with sufficient overall accuracy using a current sensor (e.g., a shunt type resistor or employing the Hall effect) capable of measuring high electric currents (hundreds of amperes or more). The large size of current sensors, however, would make it extremely difficult to embed one into a battery as part of a battery-monitoring unit. Another serious problem is the high cost of current sensors.

There were three targets with the intelligent battery. The first target was to provide the algorithm which does not need a current sensor to monitor battery states. The second target was to develop a monitoring unit of battery states with an automatic alarm and an optical data transfer system. With this alarm function, a driver need not check a battery until an alarm alerts to a degradation problem. The third target was to develop a data acquisition instrument which receives more detailed data from the optical data transfer system of the monitoring unit. In this report, the research and development

* Corresponding author. Tel.: +81 48 546 1113; fax: +81 48 546 1137.
E-mail address: keizo.yamada@shinkobe-denki.co.jp (K. Yamada).

0378-7753/$ – see front matter © 2008 Elsevier B.V. All rights reserved.
doi:10.1016/j.jpowsour.2008.06.092

Nomenclature

I	current (A)
I_{st}	current corresponding to V_{st} (A)
K_t	temperature correction factor of electrical load of vehicle
OCV	open circuit voltage (V)
OCV^0	open circuit voltage of new battery (V)
r	internal resistance of conventional battery (Ω)
r^0	internal resistance of new battery (Ω)
R	electrical load of vehicle (Ω)
SOC	state of charge (%)
SOH	state of health (%)
T	Temperature (°C)
V_{st}	minimum voltage at engine start-up (V)
V_{st}^0	minimum voltage at engine start-up with new battery (V)
W	output power (W)

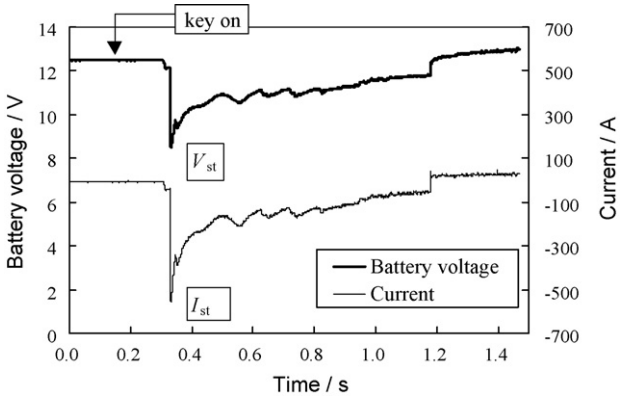

Fig. 1. A voltage profile and current profile of a battery at engine start-up.

leading up to the completion and commercial release of CYBOX® are described.

2. Theory

2.1. Model

Battery degradation is evaluated by measuring the engine start-up voltage (V_{st}), the minimum voltage to which a battery drops when a driver starts the engine of a vehicle (see Figs. 1 and 2). Though the coil of a starter motor is in the current pass in a vehicle,

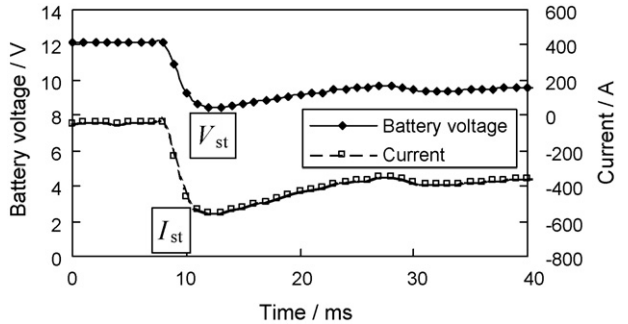

Fig. 2. An extended figure of Fig. 1 at a finer time resolution to show rapid changes in the voltage and electric current.

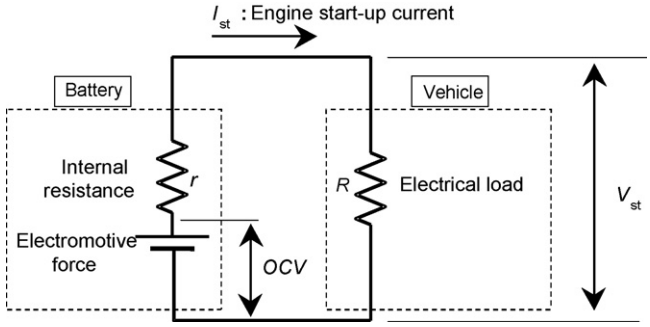

Fig. 3. An equivalent circuit of the problem.

the engine start-up voltage V_{st} can be expressed as an equivalent circuit (see Fig. 3), provided that the electrical load of the vehicle can be expressed as a simple electrical resistance, R, before the starter motor starts rotating.

2.2. Formulation

This problem can be expressed in two forms, as follows.
For the vehicle side:

$$V_{st} = RI_{st} \tag{3}$$

For the battery side:

$$\mathrm{OCV} - V_{st} = rI_{st} \tag{4}$$

where I_{st} is the current when V_{st} is observed, and r is the internal resistance of the battery. By combining Eqs. (3) and (4), the following expression of V_{st} can be obtained:

$$V_{st} = \mathrm{OCV}\frac{R}{R+r} \tag{5}$$

Considering a fresh, fully charged battery in the standard conditions, Eq. (5) can be expressed as follows:

$$V_{st}^0 = \mathrm{OCV}^0\frac{R}{R+r^0} \tag{6}$$

By combining Eqs. (5) and (6), V_{st} can be expressed without determining the automotive electrical load, R, as follows:

$$V_{st} = \frac{\mathrm{OCV}}{(\mathrm{OCV}^0/V_{st}^0 - 1)r/r^0 + 1} \tag{7}$$

It is thus found that V_{st} is the function of r/r_0, the rate of increase of the internal resistance of the battery. Given that the voltage parameters OCV, OCV^0, V_{st}, and V_{st}^0 are all measurable, Eq. (7) can be used to yield information on the battery internal resistance, r/r_0, without relying on a current sensor. Calculations with V_{st} are therefore a key approach to obviating the current sensor. When the estimations of internal resistance are based on the voltage after the starter motor starts rotating, the current depends on unpredictable mechanical loads, such as the friction of pistons in the engine. Under such conditions, it becomes difficult to extract battery conditions without a current sensor.

3. Results and discussion

3.1. Hardware of the battery-monitoring unit

Fig. 4 shows a circuit block diagram of the battery-monitoring unit. The unit has a high voltage resolution of 20 mV for high measurement accuracy of OCV and V_{st}, and a short sampling interval of 2 ms to avoid missing the minimum voltage during measurement

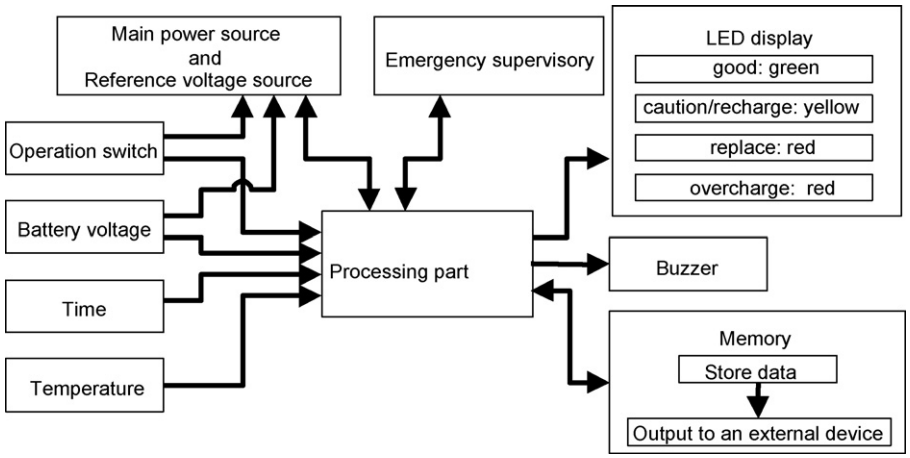

Fig. 4. Circuit block diagram of the battery-monitoring unit.

of V_{st}. For reduced consumption of battery power by the electronic circuits, the battery-monitoring unit incorporates an auto power start circuit to maintain a power-off state until the battery goes into service. The current consumption during the power-off state is less than 20 μA. When a battery is installed in a vehicle, the battery-monitoring unit will detect a voltage change, automatically judge that the battery is installed, and issue instructions to switch the electronic circuit into an operational mode.

Fig. 5 shows a battery-monitoring unit incorporating the electronic circuit described above. The case measures 100 mm in length, 40 mm in width, and 20.5 mm in height, at maximum. The mounted PCB (printed circuit board) is molded with resin to strengthen the water resistance, acid resistance, and anti-vibration performance. Connecting parts inserted into the positive and negative battery terminals are fashioned as bus bars of the integral molding, as a another strategy to protect the circuits against vibration. The battery-monitoring unit is embedded into a concave portion of the battery lid.

3.2. Functional features

These technologies are applied to a series of 12 V automotive intelligent batteries (CYBOX®). An overview of CYBOX® follows.

3.2.1. Diagnostic operation

Fig. 6 shows the operations of the battery-monitoring unit embedded into the battery. The diagnostic operation has two functions: first, the issuance of an automatic alarm (CYBOX® buzzes to automatically notify a driver of the battery conditions); second, a manual check to display the diagnostic results for a user at the push of a button on the battery. The diagnostic results are "good," "recharge," "caution," "replace," and "overcharge." When the battery condition is not "good," the battery-monitoring unit will sound a beep for about 30 s after the engine stops. The diagnostic result "caution" tells a driver that the battery deterioration has reached a certain level. The automatic alarm function for "caution" stops when the driver notices the beep, recognizes the "caution" result, and pushes the button on the battery. The manual check function allows a driver to check battery conditions at any time by pushing the button on the battery. The manual check function is auxiliary to the automatic alarm function.

3.2.2. Data acquisition instrument

An optical data transfer system, which is embedded into the battery-monitoring unit, was developed. This optical data transfer system uses the LEDs which are usually used for displaying battery conditions. Various data collected from the battery from the point of vehicle startup are stored in a nonvolatile memory. Much of this data, for example, the engine start-up count, can be read by a data acquisition instrument (see Fig. 7).

3.2.3. Battery design for the built-in battery-monitoring unit

To protect the bus bar from liquid corrosives (for example, the sulfuric acid that tends to leak through the top vents of conventional batteries covered with plugs), CYBOX® is equipped with a manifold cover with vents on the sides of the battery.

The schematic view in Fig. 8 shows the battery cover with parts detached for illustrative purposes. The battery vents are posi-

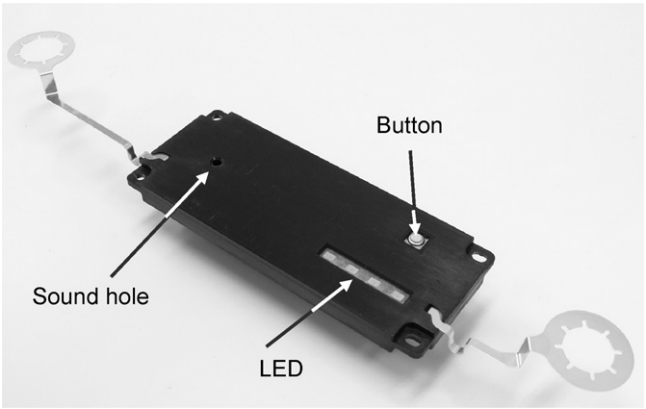

Fig. 5. A battery-monitoring unit.

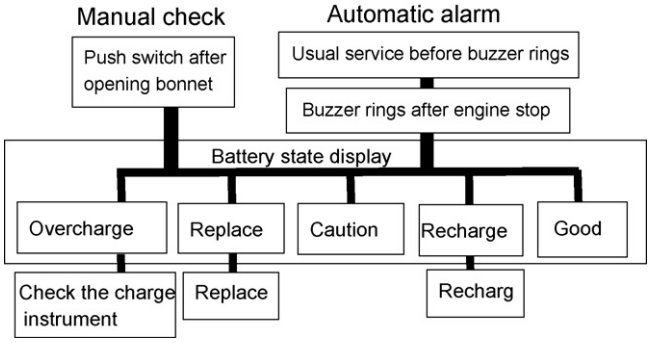

Fig. 6. Operations of the battery-monitoring unit embedded into the battery.

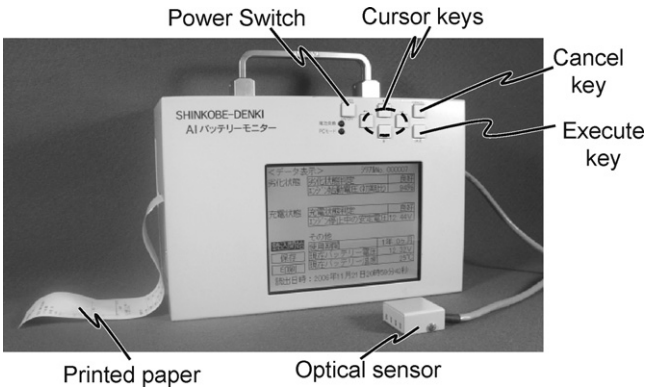

Fig. 7. A data acquisition instrument for the automotive intelligent battery.

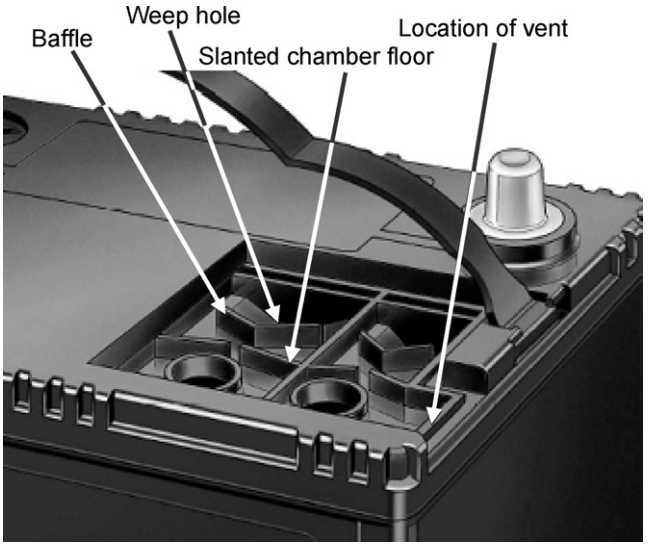

Fig. 8. A schematic view of the battery cover with parts broken away for illustrative purposes.

tioned at two points at opposite ends of the battery cover, and flame arresters made from polypropylene frit are attached behind the vents to shield the battery from external ignition sources. The manifold cover reduces water loss so effectively, the task of refilling water is eliminated throughout the service life. The movement of water between cells due to differentials in water vapor pressure caused by variations of the temperature and acid concentrations between the cells was also demonstrated to be non-critical.

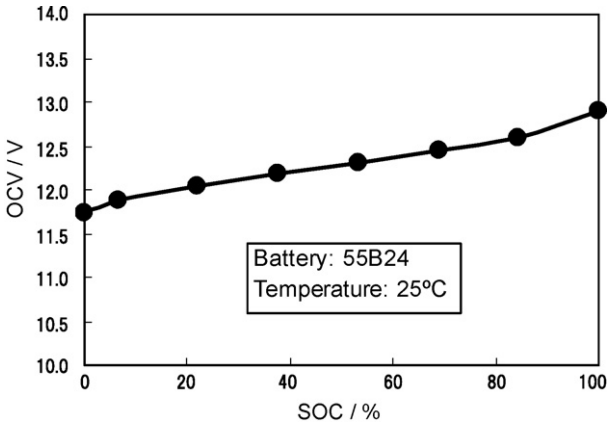

Fig. 10. The relationship between SOC and OCV for an automotive battery (55B24).

An external view of the battery with the built-in battery-monitoring unit is shown in Fig. 9. This product was released on the Japanese market from August 2004 as the intelligent automotive battery CYBOX®.

3.3. The battery-monitoring technology

3.3.1. SOC diagnostic procedure

Fig. 10 shows the relationship between SOC and OCV for an automotive lead-acid battery (55B24). When SOC changes from 100% to 0%, the variation of OCV is about 1.2 V. In practice, the required precision of SOC will be 10% or less. Given the variation per SOC 10% of about 120 mV, the hardware of the battery-monitoring unit must therefore be able to measure voltage with an accuracy of less than 120 mV. The time required for the stabilization of OCV after a charge or discharge is another factor. Before the battery-monitoring unit measures OCV, it must account for this time by recognizing, first, that the engine is stopped, and second, that OCV has fully been stabilized. Fig. 11 shows the OCV profile of a battery with a SOC 100% SOC, just after overcharging. When the battery is overcharged, it takes several hours for OCV to stabilize. In Fig. 11 it takes about 3 h.

Fig. 9. An external view of the battery with the built-in battery-monitoring unit.

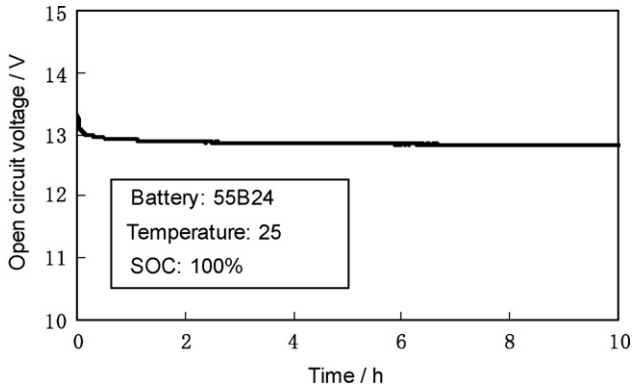

Fig. 11. An OCV profile of a battery at SOC 100% after overcharging.

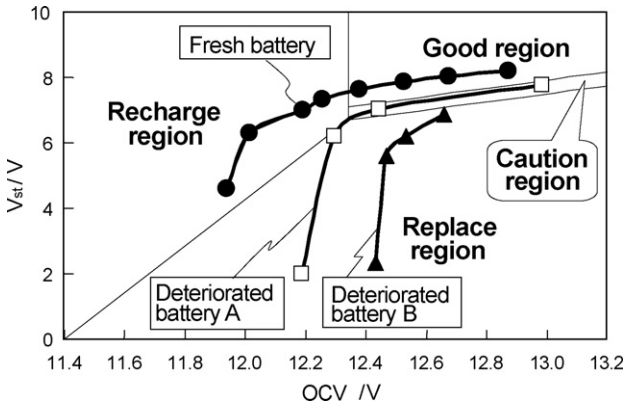

Fig. 13. A V_{st}–OCV map with plots of V_{st} versus OCV measured for a new battery and two deteriorated batteries with different degradation states.

3.3.2. Procedure for diagnosing deterioration

To evaluate deterioration, it is required to choose a parameter correlated with the direct-current internal resistance. In this study the engine start-up voltage, V_{st}, was adopted as a parameter correlated with the internal resistance, as described in section 2. Experience shows that the voltage drop of a battery at engine start-up becomes more severe as the battery degrades and the direct-current internal resistance climbs. Fig. 1 shows a voltage profile and current profile of a battery at engine start-up. The battery voltage drops immediately at startup, then rises in an oscillating fashion. The oscillation of an electric current synchronizes with the oscillation of the voltage. Complete engine start-up is reached in less than one second. The minimum voltage in Fig. 1 is defined as the engine start-up voltage, V_{st}, and the current corresponding to V_{st} is defined as the engine start-up current, I_{st}. Fig. 2 plots the same data shown in Fig. 1 to show the rapid changes in the voltage and electric current at a finer time resolution (data-sampling interval: 1 ms). In Fig. 2, the time up to V_{st} and I_{st} appears to be about 4 ms. Since the part of the voltage curve at the timing of the V_{st} measurement is broad more than 2 ms, the sampling interval of the battery-monitoring unit was designed to be 2 ms.

Based on the electrical circuit designation of V_{st}, Fig. 3 shows the relationship of the equivalent circuit during an engine start-up with V_{st}, OCV, and r. The parameter R, the electrical load of the vehicle, is assumed to be constant. According to Eq. (5), the voltage at engine start-up, V_{st}, is a function of OCV, the direct-current internal resistance of a battery, r, and the electric load of a vehicle, R. Fig. 12 shows the electric load of a vehicle calculated from Eq. (3), substituting experimental values for V_{st}, and I_{st}, based on measurements for various SOCs using eight deteriorated batteries with different SOHs. From Fig. 12, it can be confirmed that the electrical load of a vehicle at engine start-up, R, remains nearly constant irrespective of battery conditions. This is an important point to confirm, as it is difficult to ascertain a definition for the relationship between V_{st} and the parameters of battery conditions when R, the electric load of the vehicle, is dependent on battery conditions. If it were impossible to confirm the constant state of the electric load, therefore the use of V_{st} as an indicator of battery conditions would have to be forgone. The engine start-up voltage V_{st} is dependent on OCV and the internal resistance r. Given that OCV and the direct-current internal resistance r depend on SOC and SOH, respectively, and further, that these dependencies are predictable at some level, V_{st} turns out to be a practical parameter for showing battery conditions. And in addition to reflecting the direct-current internal resistance r, the parameter V_{st} is directly related to the output power ($W = V_{st}, I_{st}$) to the starter motor, a factor important for the engine start-up performance of a vehicle. Though SOH could be estimated by computing the rate of internal resistance, r/r_0, from Eq. (7), instead of r/r_0 or SOH, V_{st} is used as an indicator for diagnosis of the engine start-up performance in this study.

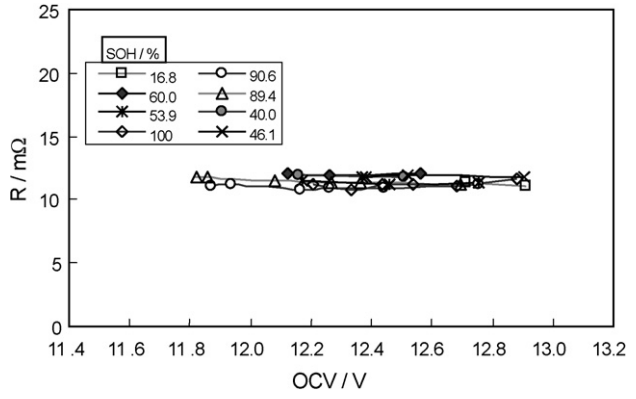

Fig. 12. The electric load of a vehicle calculated from Eq. (3) substituting experimental values to V_{st} and I_{st}.

3.3.3. Diagnosis of battery conditions by V_{st}–OCV map

A V_{st}–OCV map can be used to diagnose battery conditions. Fig. 13 shows the plots of V_{st}, versus OCV, measured for a new battery and for two deteriorated batteries with different degradation states, on a V_{st}–OCV map. The temperature of these batteries were the standard temperature, 25 °C.

This V_{st}–OCV map is divided into four regions for the diagnosis of battery conditions: the good region, the caution region, the replace region, and the recharge region. The boundary lines between the regions were determined based on the relationships of OCV and V_{st} in about 128 sold batteries at different SOHs, measured either during use or after use. The goal in boundary placement was to avoid no-start trouble before the battery-monitoring unit alarms issued a "recharge" or "replace" alarm. According to an investigation of several vehicles, the threshold of V_{st} to startup failure is less than 6 V for vehicles of 1500 cm^3 class or larger. Thus, all of the plots under the line of $V_{st} = 6$ V had to be located in either the "replace" or "recharge" region. Furthermore, the plot in the fully charged state had to be located in the "replace" region for all of the batteries with V_{st} plotted at less than 6 V in the "replace" region. In the "replace" region, V_{st} will sharply decrease if OCV declines for longer than a certain period, and ultimately fail at engine startup. A battery in the recharge region may return to the good region if it is recharged and OCV increases. In tests to verify the validity of each region, it was found out that the regions were well positioned. The boundary of the regions might differ for batteries from different manufacturers.

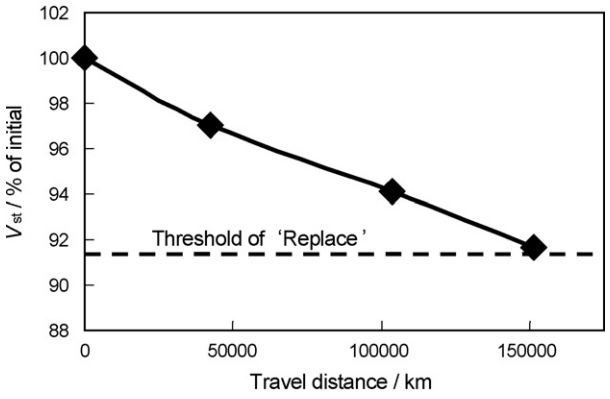

Fig. 14. An example of field data showing V_{st} profile of 65B24 CYBOX® in a commercial vehicle.

Before applying a set of V_{st} and OCV values to the V_{st}–OCV map, V_{st} was compensated with temperature in consideration of the temperature dependencies on both the electrical load of the vehicle and the battery's internal resistance.

The compensation of V_{st} for the temperature dependence of battery's internal resistance was achieved with the temperature correlation factor which is based on experimental data of V_{st} at various temperature of the battery.

The temperature dependence of an electrical load at an engine start-up, R, is also taken into account, assuming that R can be approximated by an electric resistance of the electrical parts made from copper such as a coil in a starter motor. The compensation of V_{st} for the temperature dependence of the electrical load of a vehicle can be done with the following expression.

$$V_{st}|_{t=20^\circ C} = \mathrm{OCV}\frac{V_{st}K_t}{V_{st}K_t + \mathrm{OCV} - V_{st}} \quad (8)$$

where K_t is a temperature correction factor [8] of an electrical load of a vehicle.

The engine start-up performance of the installed battery can be diagnosed with high accuracy by applying computations based on the electrical load R. Once a battery is put into service, V_{st}^0 is measured and memorized, then a V_{st}–*OCV* map is prepared. Given that the electrical load R changes in every vehicle, V_{st} also changes from vehicle to vehicle, even when the same battery is installed (see Eq. (5)).

Fig. 14 is an example of field data showing V_{st} profile until the monitoring unit alarms "replace" for 65B24 CYBOX® in a commercial vehicle. V_{st} decreased straightly and it can be found that the algorithm works as expected.

4. Conclusions

A new algorithm was developed for battery diagnostics without a current sensor. By eliminating the need for a current sensor, a battery-monitoring unit was able to be designed small enough to fit into a battery. The intelligent automotive battery, CYBOX®, is currently produced commercially. Conclusions are summarized as follows.

(i). A small monitoring unit of battery states with an automatic alarm and an optical data transfer system was successfully developed.
(ii). A theoretically supported algorithm for the monitoring unit of battery states, having no parameter of current, was developed in terms of the map of V_{st} versus OCV.
(iii). The data acquisition instrument which receives more detailed monitored historical data from the optical data transfer system of the monitoring unit was developed.

Acknowledgements

The authors are thankful to Mr. Tokiyoshi Hirasawa, the deputy general manager of R & D division in Shin-Kobe, for his generous guidance. The authors' thanks are also due to Mr. Takashi Kofuse (Shin-Kobe), Mr. Takashi Hara (Shin-Kobe), Mr. Kenichiro Tsuru (Hitachi Vehicle Energy), and Mr. Akihiko Kudo (Hitachi Vehicle Energy) for their helpful advice.

References

[1] D. Berndt, Maintenance-Free Batteries, 2nd ed., Research Studies Press Ltd., Somerset, England, 1997, pp. 86–93, 438.
[2] D.A.J. Rand, P.T. Moseley, J. Garche, C.D. Parker (Eds.), Valve-regulated Lead-acid Batteries, Elsevier, Amsterdam, Netherlands, 2004, p. 207.
[3] N. Ohkubo, S. Kishida, S. Ito, T. Kawai, K. Kikuchi, T., Kikuchi, US Patent 6,621,250 (16 September 2003).
[4] S. Piller, M. Perrin, A. Jossen, J. Power Sources 96 (2001) 113.
[5] D.O. Feder, T.G. Croda, K.S. Champlin, S.J. McShane, M.J. Hlavac, J. Power Sources 40 (1992) 235.
[6] T. Okoshi, K. Yamada, T. Hirasawa, A. Emori, J. Power Sources 158 (2006) 874.
[7] T. Teratani, J. IEEJ 122 (2002) 356.
[8] IEC 60228, conductors of insulated cables, 2004.